PRELIMINARY IMPLEMENTATION OF HIBP FOR HSX BASED UPON ELECTRIC FIELD EFFECTS

by

MICHAEL A. BINGHAM

A Thesis Submitted to the Graduate

Faculty of Rensselaer Polytechnic Institute

in Partial Fulfillment of the

Requirements for the degree of

MASTER OF SCIENCE

Major Subject: Electrical Engineering

Approved:

_____
K. A. Connor, Thesis Adviser

Rensselaer Polytechnic Institute
Troy, New York

May 2008

CONTENTS

LIST OF TABLES

LIST OF FIGURES

ACKNOWLEDGMENT

ABSTRACT

Completion of a design study on the reconstruction of the electric field $\vec{E}$ in a magnetically confined plasma by means of the deflection of a non-confined heavy ion beam has proven concept viability and prompted specific application of heavy ion beam probe technology (HIBP) to the Helically Symmetric eXperiment (HSX). Significant work was undertaken in the deconstruction of the Rensselaer Plasma Dynamics Laboratory (RPDL) HIBP and its preparation for application to HSX. The measurement is based upon the path integral effects the electric field $\vec{E}$ acting on a particle passing through a plasma where the magnetic field $\vec{B}$ is well known. As with standard HIBP technology it is feasible to alter the beam energy and injection angle allowing for the sampling of various regions within the plasma under study. It is possible to measure the deflection in the trajectory of the particle by means of a detection grid and obtain information about the plasma allowing for the reconstruction of the electric field $\vec{E}$. Previous study has demonstrated that reconstruction based on this technique is reasonable so long as $\vec{E}$ is sufficiently strong, being on the order of 1 percent of $\vec{v} \times \vec{B}$, where $\vec{v}$ is the velocity of the subject ion and $\vec{B}$ is the confining magnetic field. Major simplification is realized in the application of this diagnostic via the substantially lower ion accelerator voltages as compared to standard HIBP technology.

1. INTRODUCTION

Situated in Engineering Hall on the Madison campus of the University of Wisconsin, the Helically Symmetric eXperiment (HSX) is a unique concept in fusion research. Operated by the Electrical and Computer Engineering department, the project aim is to bring together the best aspects of tokamak and stellarator plasma fusion technology. This is accomplished by optimizing the geometry of the modular coil stellarator for a Quasi-Helically Symmetric (QHS) configuration [1]. Often the unique shape of the vacuum chamber is described as a warped donut which is in turn surrounded with large distorted copper coils.

Obtaining detailed information about the magnetic surface structure is essential to the operation of HSX, allowing assessment of the QHS configuration. A good electric field $\vec{E}$ diagnostic will enable a more complete identification of benefits of QHS. The Heavy Ion Beam Probe (HIBP) is historically proven as an adaptable and extremely accurate plasma diagnostic device for the measurement of electric potential ϕ. Knowledge of the plasma potential profile and of the containing magnetic field allows the reconstruction of the electric field $\vec{E}$ [2].

Standard HIBP technology makes use of high accelerator voltages which requires significant care to be taken in gun design and safety. Further the standard technology requires large ports, or openings, into the vacuum vessel to allow for a wide range of beam injection angles and secondary trajectories which must enter the large energy analyzer apparatus. Though standard HIBP techniques require a bulky set up to be integrated into the plasma device significant simplification is possible.

Practical efforts were devoted to the relocation of the Rensselaer Plasma Dynamics Laboratory (RPDL) HIBP in Troy, NY to the HSX group in Madison, WI. Significant time was devoted to the rebuilding of the system at HSX to enable its future application as a diagnostic.

This research is a continuation of previous efforts to develop a simplified electric field diagnostic for HSX. Many techniques that were originally developed and vetted for standard HIBP can be adapted for specific use on HSX. Through the use of practical

geometric and field models a new approach for the reconstruction of the electric field $\vec{E}$ is investigated.

It is appropriate to briefly describe HSX and develop a basic framework for the operation of standard HIBP. Then the new application of HIBP to HSX can be presented and comparison to the older techniques noted. Work completed in the relocation and reconstruction of the RPDL HIBP to HSX will be detailed in chapter two. Further the formal procedures developed for system operation are detailed. The third chapter details predicted deflections in Cs 133 ion trajectories launched from a 10kV beam in a reduced model with fields based on those in HSX. Focus on the heavier Cs ion and lower accelerator voltages are founded upon earlier work conducted by RPDL members as these parameters have shown the best ability to sample a wide variety of locations in HSX. Explanation of simulation methodology and results is also detailed. Last a modified method for reconstructing the electric field in HSX by trajectory deflection is suggested for future investigation.

1.1   Helically Symmetric eXperiment (HSX)

Located in Engineering Hall and run by the Electrical and Computer Engineering department at the University of Wisconsin, HSX is a medium sized modular coil stellarator. The device has been optimized for a quasi-helically symmetric (QHS) configuration and represents a unique concept in stellarator design. The warped shape of the toroidal vacuum vessel is mirrored in the distorted forms of the copper coils surrounding it. Figures 1.1 and 1.2 provide a visual augment as well as high level system identification [3]. Figure 1.2 gives a very clear view of a box port, at left, much like the one that will eventually accept the HIBP system. The essential parameters of HSX are summarized below in table 1-1. The major research objectives, as stated in the physics goals for the project, of HSX are transport, turbulence, QHS confinement, and vessel wall conditioning [4].
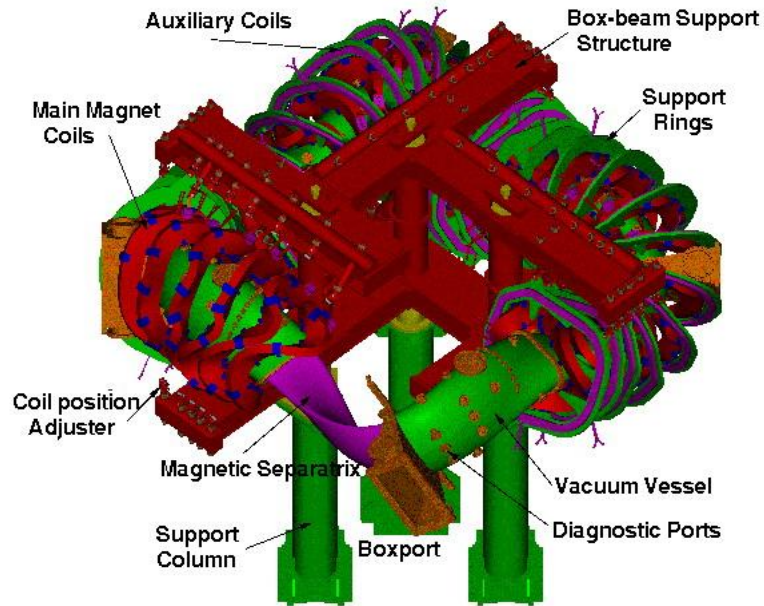
Figure 1.1 – CAD Depiction of HSX with Major Structures Labeled
http://www.hsx.wisc.edu/construction.shtml
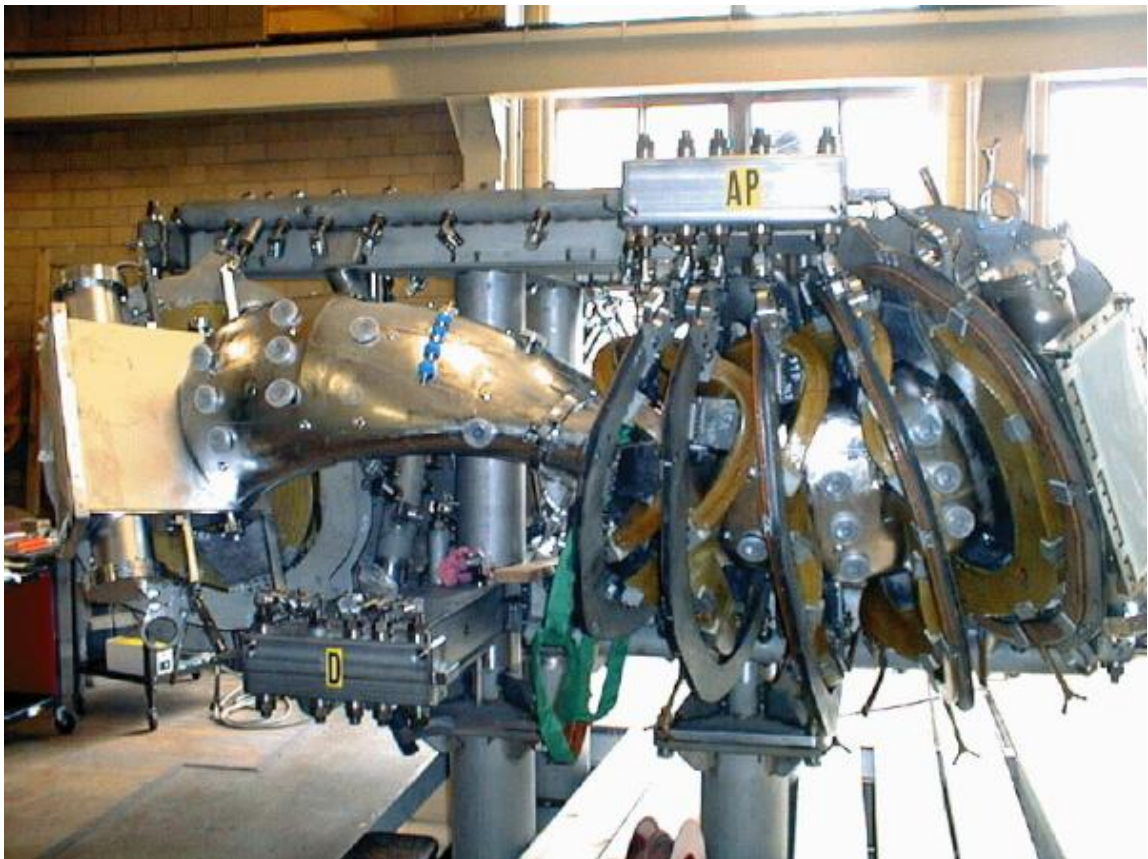
Figure 1.2 – HSX During Construction: Box Port & Vacuum Vessel Visible at Left
http://www.hsx.wisc.edu/pictures/construction/

The HSX program is a unique evolution in stellarator design in seeking to bring together the best attributes of stellarator and tokamak technologies; by giving the confinement properties of energetically efficient tokamaks to the inherently stable stellarator. This has been made possible by optimizing geometry for QHS and this has dictated the strange shape of the device.

Tokamak based fusion experiments have achieved the best results to date, but their requirement for large plasma currents to generate the components of magnetic field $\vec{B}$ necessary for containment leaves them vulnerable to disruption and it is not clear if it will be possible to drive or control such large currents in reactor sized machines. Further these are devices operated in a pulsed mode and that is not the ideal operation mode for a future fusion power plant, due to the requirement for long operating lifetimes and the hazard of cyclic fatigue induced mechanical stress.

Since stellarators do not require plasma current to produce the confining component of the magnetic field $\vec{B}$ they do not have tokamak type current limitations and are free from the disruptions of pulsed operation as well; however, they suffer from transport losses and lose energy at a relatively high rate. In past designs ripple induced in the magnetic field by the coils tended to trap some plasma and lead to these high losses. The QHS optimization enables confinement without such high energy loss by significantly reducing transport. Essentially HSX is equivalent to a tokamak without the plasma current.

The QHS is achieved by using sets of modular coils to produce the magnetic field $\vec{B}$. The coils were designed so that there is essentially no toroidal curvature in the confining magnetic field and the QHS improves single particle confinement as compared to other stellarator designs [1]. Further, HSX has a very small aspect ratio $A = \dfrac{R}{a} = 8$ where R is the major radius and a is the minor radius of the device [4]. To achieve this near symmetry a standard toroidal device would require an aspect ratio of nearly 400, a monster of a machine [1]. In HSX the confining magnetic field $\vec{B}$ is generated independently of the plasma and it is effectively the same inside and out side of the plasma making it a low β device, where β describes the ratio of plasma pressure

4

to magnetic pressure. Consequently, HSX is a device well suited to an ion beam diagnostic for the electric field $\vec{E}$ as $\vec{B}$ is well know throughout the device and the influence of the force component due to $\vec{E}$ of the plasma alone on the ion trajectories can then be measured.

Construction of a radial electric field profile is essential for HSX as one of the major research objectives is the study of transport and confinement. Knowledge of the radial electric field is crucial to understanding these phenomena and can eventually be used to determine how much symmetry in the coils is required to realize low transport rates. Ultimately engineering of the coils may be simplified and techniques learned from HSX can be adapted for a commercial fusion reactor.

Table 1-1: HSX Device Parameters [4]

Major Radius (machine center to Plasma center - avg.):	1.20 meters
Average Plasma Minor Radius:	0.15 meters
Aspect Ratio (Major Radius/Plasma Radius):	8
Plasma Volume:	0.44 cubic m
Number of Field Periods (symmetry around torus):	4
Rotational Transform (magnetic field torsion): on Axis :	1.05
Edge:	1.12
Magnetic Well Depth:	0.6 %
Number of coils/Field Period:	12
Average Coil Radius:	0.30 meters
Number of Conductor Turns / Coil:	14
Coil Current (maximum):	13.4 kiloA
Magnetic Field Strength (maximum):	1.37 Tesla
Magnet Pulse Length (full field):	0.2 seconds
Auxiliary Coils /period:	12

1.2 Fundamental Concepts of HIBP Technology

1.2.1 Introduction & Brief History of HIBP

The Heavy Ion Beam Probe (HIBP) is an adaptable and proven plasma diagnostic device, with primary application to magnetic confinement fusion experiments. Though originally conceived of by Robert Hickok and Forest Jobes in the late 1960's to measure poloidal magnetic field values the practical difficulty of this measurement prompted device development along different avenues. The measurement of electric potential ϕ within the plasma quickly emerged as the most important use of the HIBP. Further diagnostic abilities of the device include the ability to measure electron density n_e, electron temperature T_e, and magnetic vector potential $\vec{A}$.

Possessing diagnostic ability over a wide range of plasma conditions has made the HIBP a very flexible diagnostic device. This adaptability has lead to research on the HIBP not only in the United States, but also in the former Soviet Union since the early 1970's and in Japan since the start of the 1980's on a number of different types of devices. As of 2002 there were approximately a half dozen [5] HIBP's operating on a Varity of magnetic confinement devices including: Tokamaks, Stellarators, and Reversed Field Pinches (RFP).

Development of the HIBP in the United States has been, essentially, the sole domain of the group at the Rensselaer Polytechnic Institute's Plasma Dynamics Laboratory (RPDL). Work at the RPDL has spanned more than thirty years and resulted in the successful installation and experimentation of the HIBP on six different plasma confinement devices [3]. The program has been involved with the Rentor Tokamak, Elmo Bumpy Torus (EBT), Tandem Mirror Experiment (TMX), Texas Experimental Tokamak (TEXT), Advanced Toroidal Facility (ATF), and most recently the Madison Symmetric Torus – RFP, and the HSX program.

1.2.2 Principles of HIBP Operation

Distilled to its basic premise, the HIBP is a type of test particle experiment. That is, information about the plasma under study is derived from the action taken on a

specific species of ion. Consistent with the name HIBP, heavy ions from the type IA elements are most commonly employed as the test particles.

In the traditional experiment a beam of singly charged ions, termed primaries P^+, are introduced across the magnetic field $\vec{B}$ into the plasma under study. Passing through the plasma the primary ions, or test particles, may undergo further ionization to state P^{n+1}. Often these are doubly charged particles P^{+2}, called secondaries, and are subsequently detected and analyzed outside the plasma. The ionization allows for separation of primaries and secondaries based on their difference in charge [2]. Recall the Lorentz Force is given as:

$$\vec{F} = \vec{F}_e + \vec{F}_m \qquad\qquad 1.1$$

$$\vec{F} = q\vec{E} + q\left(\vec{v} \times \vec{B}\right) \qquad\qquad 1.2$$

A direct implication of 1.2 is that a change in the charge (q) on the particle results in a different force felt by the primaries and secondaries. Thus the trajectories traced out by the test particles will depend on their states of ionization, see figure 1.3 below. These concepts are illustrated in Figure 1.3 and note that the different ionization sites within the plasma determine the initial points of the secondary trajectories. This means that only secondaries ionized at specific locations within the plasma will reach the detector. In this way a sample volume is defined and measurements are localized to the ionization position [2].

In order to change the sample volume the primary ion beam is steered by means of electrostatic deflection via the sweep plates. For the system to be implemented on HSX beam focus is also achieved using this same principle. Since the dominant collision process present in HSX is electron impact ionization [2], it is possible to say that the initial momentum of the secondary is approximately the same as the momentum of the primary at the point of ionization.
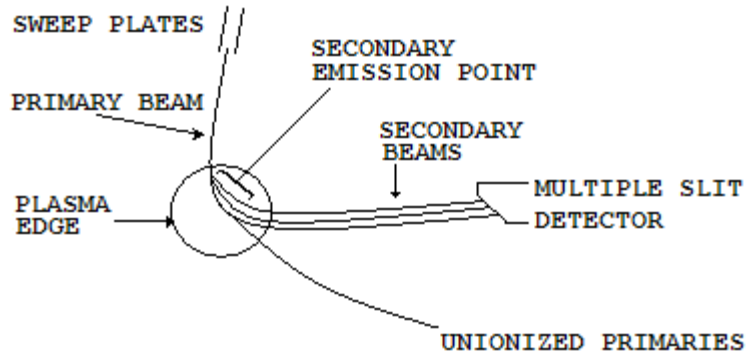
Figure 1.3 Test Particle Operation of the HIBP

Critical to the design of a HIBP system is the ability of the secondaries to arrive at the detector. Thus they must escape the magnetic field $\vec{B}$ which contains the plasma. To a good first order approximation this condition can be met by setting the Larmor radius r_L, or gyromagnetic radius, of the ion to be detected equal to the minor radius of the plasma (a) [6]. If the curvature of the trajectory were more extreme it could become trapped in the field region and continue to spiral around without ever reaching the detector.

$$\text{Larmor Radius} \equiv r_L = \frac{Mv}{q_s B} = a \qquad\qquad 1.3$$

M = ion mass
q_s = charge of secondary ion
v = magnitude of ion velocity
B = magnitude of magnetic field
a = minor radius of the plasma

Equation 1.3 allows for the design of a HIBP experiment based on the estimation of how extremely an ionized secondary will curve. If the curvature is too extreme, the Larmor radius being less than the minor radius of the plasma, the ion will spiral within the plasma and be unable to reach the analyzer. Casting the argument in terms of plasma parameters it is possible to set the following condition on ion properties:

8

$$\frac{MW_b}{q_s^2} > \frac{a^2 B^2}{2}$$

$$W_b = \text{beam energy}$$

<div align="right">1.4</div>

The most important result of this relation is the need to maximize the left hand side to ensure ion escape. Thus large beam energy W_b and ion mass M are desired. This is why the device is known as a heavy ion beam probe; using relatively massive type IA elements in many experiments. The most commonly employed ions in past experiments have been: Li, Na, K, Rb, Cs, or Ti which are all heavy compared to the plasma particles [7]. It is common for beam energies to range widely from 10KeV up to 2MeV [2].

In HIBP experiments it is common for the initial position of the beam, called the sweep point, and the location of the detector to be fixed by physical considerations. Plasmas are contained within vacuum chambers and ports into this environment are at a premium. Further the location of magnetizing coils and reactor structure will severely limit injection and detection sites. Consequently the ability to sample different plasma volumes is primarily a function of beam energy and angle [2].

1.2.3 Electric Field Measurement

Measurement of the electric potential ϕ is exceedingly important because it offers direct insight and understanding of the confined species. In a magnetically confined device the plasma is said to be quasi-neutral; however, the different mobilities of ion and electron species results in different rates of loss from the plasma. Since the mobility of the electron is so much greater than that of the ion it results in the rapid loss of electrons from the plasma. This in turn causes the plasma to develop a positive charge imbalance.

The HIBP is capable of making non-perturbing measurements of the plasma potential profile in high temperature plasmas. This particular measurement is based on the conservation of energy and requires that the beam energy of the injected and detected species be well known [5]. Prior to entering the plasma the injected ion has purely kinetic energy. Upon entering the plasma it experiences the potential energy due to the

charge distribution existing within the plasma. The key point is that the sum of kinetic and potential energies, of the particle, is conserved as it passes through the plasma.

In order to simplify analysis, it is assumed that any time derivative of the magnetic vector potential is very small and is negligible in influence reducing the electrostatic field to $\vec{E} = -\nabla\phi$. The sweep point and detector are considered at ground potential and the beam enters the plasma with an initial energy of W_i, but may also be given in terms of the product of gun voltage V_g and the charge on the primary ion q_p. The particle then passes into and through the plasma, with constant total energy. That is the sum of kinetic and potential energies is a constant. Upon reaching the ionization point electrons with potential energy of $-e\phi_{sv}$ are removed, e being the elementary charge. The electrostatic potential of the sample volume is called ϕ_{sv}. Then the total energy of the secondary ion is given by [2]:

$$W_d = W_i + (q_s - q_p)\phi_{sv}$$ \hfill 1.5

q_p = charge on the primary ion
q_s = charge on the secondary ion
W_d = beam energy at detector

Since energy is conserved as the ion passes out of the plasma and reaches the energy analyzer detector it is possible to solve for ϕ_{sv} and the plasma potential from [2]:

$$\phi_{sv} = \frac{W_d - W_i}{q_s - q_p}$$ \hfill 1.6

Note this is the plasma potential localized to the sample volume as there is no way to know about regions of the plasma where the ion beam has not reached. Standard HIBP set ups have made measurements in plasma potential on the order of tens of volts using accelerator voltages in the hundreds of kilovolts. Comprehensive electric potential

radial profiles have been developed for devices where other diagnostics methods have proven unable to obtain such data [8].

The potential measurements performed by HIBP provide a means of obtaining the electric field. The major simplification, as previously stated, neglects the time derivative of magnetic vector potential. The electric field is then directly obtained by taking the negative of the gradient of potential. This simplification is stated explicitly in equation from below:

$$\vec{E} = -\nabla\phi - \left.\frac{\partial\vec{A}}{\partial t}\right|_{\frac{\partial\vec{A}}{\partial t}\cong 0} \qquad\qquad 1.7$$

$$\vec{E} = -\nabla\phi \qquad\qquad 1.8$$

1.3 New Diagnostic Technique for HIBP

The conditions present in HSX permit the application of a new HIBP approach in obtaining the electric field. That is not to say that standard HIBP techniques would fail to obtain the desired information. Rather, the specific conditions present enable the use of a modified technique which tracks deflections in a beam of primary ions. These specific conditions are inherent in the stellarator approach to plasma confinement. Most importantly, the magnetic field is essentially independent of the plasma confined. The magnetic field is very complex, but is also well known and can be switched on even when no plasma is present. Thus electric field based deflections in ion trajectories can be easily observed by comparing the trajectories of ions run through the HSX magnetic field when plasma is present and when no plasma is present. A major advantage of this new HIBP technique is that it does not require the standard energy analyzer or the ionization of the primaries to secondaries. Removal of the energy analyzer represents major simplification in the implementation of the HIBP system for HSX as well a significant reduction in cost. Primary detection has been employed in the past, but only as a means of aligning the ion beam. The largest drawback to this approach is the

increase in noise at the detector due to unwanted incidence of plasma particles, a problem not encountered in standard HIBP where energy analyzers are employed.

The basic principle is to use only the primary ion beam and to gather information about the plasma based on the deflection of the beam. This measurement of the primary beam will result in a stronger output signal, as only a portion of the primaries were ionized to make secondaries in previous HIBP work. This allows for the use of a straightforward detection device, such as a grid, as we seek only to know the deflection in the trajectories and not the energy of the ions themselves.

The HIBP gun accelerates a primary and it is steered into the plasma by standard sweep plates. The primary ion is then deflected by both magnetic and electric forces as it traverses the plasma. After exiting the ion will then strike a detector which will give its position. This is illustrated in figure 1.4 below where the electric field alters the trajectory of an ion as compared to a trajectory with magnetic field alone.
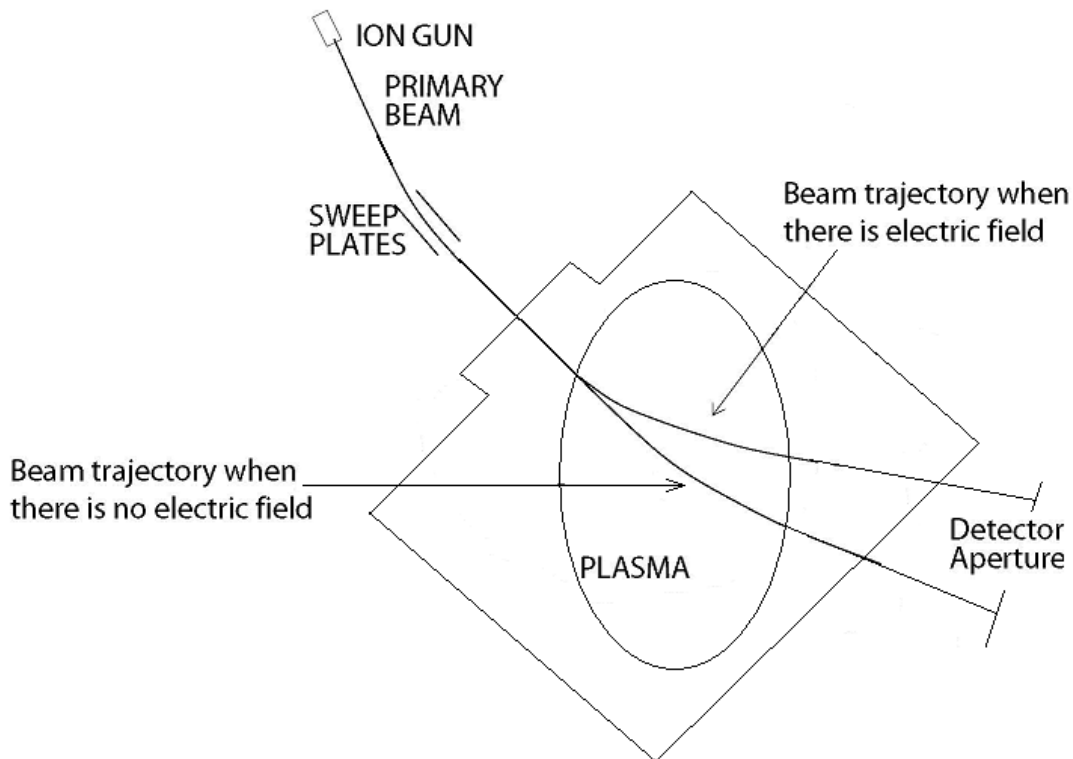
Figure 1.4 New Deflection Based Diagnostic Technique

The stellarator conditions present in HSX predetermine the magnetic field $\vec{B}$ and the plasma has essentially no influence. Since this confining magnetic filed is predetermined it is well known by design and thus magnetic field effects on the trajectory of a primary ion can be very well accounted for. Recall from equation 1.2 that the electric field will also exert a force on the charged primary ion as it traverses the plasma given as $\vec{F}_e = q_p \vec{E}$ which will result in a further deflection in the trajectory. Based on experimentally obtained information about the location of the ion at the detection aperture it is possible to reconstruct the potential whose gradient would give the electric field required to induce the observed deflection. Previous work by Chen has demonstrated that so long as $\vec{F}_e \geq (1\%)\vec{F}_m$ there will be observable deflections in trajectories [10]. This figure was based upon a layered penetration technique where electric fields were considered constant within distorted annular regions. The depth of these regions was determined by injection angle. The percentage was arrived at by predicting deflections in this HSX like geometry and considering what would be a detectable deflection in this primary detection technique. The ability to detect what may be very small electric field induced deflections will likely be limited by the susceptibility of the grid detector to noise from the plasma. Thus in real conditions a greater electric force may be required to observe deflections in ion trajectories.

2. IMPLEMENTATION OF HIBP ON HSX

2.1 Transition to Application

With the end of the helicon experiment at RPDL components of a HIBP device became available for use. Efforts were made during the summer of 2007 to verify functionality of the beam line; then once complete, the system was carefully packed up and moved to the HSX facility.

2.1.1 Summery of Objectives & Accomplishments

1. Deliver HIBP system to HSX
2. Assemble a functional beam test stand
3. Develop formal procedures of operation
4. Instruct proper HSX personnel in system operation
5. Set system baselines in beam focus and base pressure
6. Identify action areas

2.2 Preliminary Beam Line for HSX

The RPDL beam line has had several homes over the years. Originally built by Inter Science of Troy, NY in the early 1980's the system is now expected to remain with HSX as a permanent diagnostic. The goal of the work undertaken was to present the HSX group with a functional beam line test stand and to instruct key members as to the proper operation and specific procedures required to generate and steer ion beams.

The beam line is currently housed on a test stand several feet from its likely final location. The key components are depicted below in figure 2.1 and can be broken down into vacuum vessels, valves, pumps, and sensors. The vacuum vessels are chiefly the gun box, a housing with vertical adjust for the focus detection grid, two sections housing the vertical and horizontal sweep plate assemblies, and drift pipe sections. The system has two main gate valves, two solenoid valves, and three bleeder valves allowing the system to be compartmentalized. While on the test stand the beam line is pumped down via two rough pumps and two turbo pumps. Information about the state of the vacuum is obtained via two ionization gauges with thermocouples and one convectron gauge. Beam focus and position are obtained with currents induced on the wires of a detection grid.
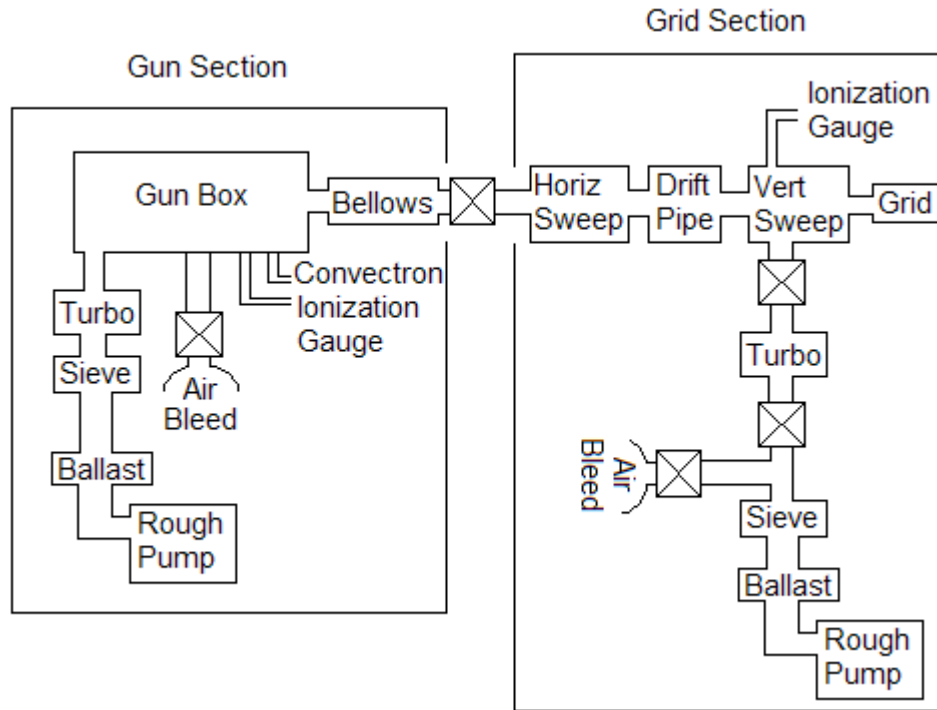
Figure 2.1 Beam Line Vacuum System Diagram

Operation of the beam line on the test stand has enabled system benchmarks and limitations to be identified prior to implementation on HSX. The limitations of the beam line fall into two major areas: hardware and detection. Hardware issues identified will need to be addressed prior to the integration of the system into HSX. Most crucial is the vacuum leak identified at the Pierce-A feed through in the gun box. This was realized after several consecutive days of pumping down yielded a base pressure of 2.6μT at the Gun Section and 0.62μT at the grid section on August 1, 2007. Leak checking with a He leak detector confirmed the placement of the breach. Further the system vacuum measurement may itself be somewhat uncertain as the only ionization gauges available to fit the available ports were quite old. However, this concern will disappear once the system is connected into the HSX vacuum and more accurate measurements will be available.

15
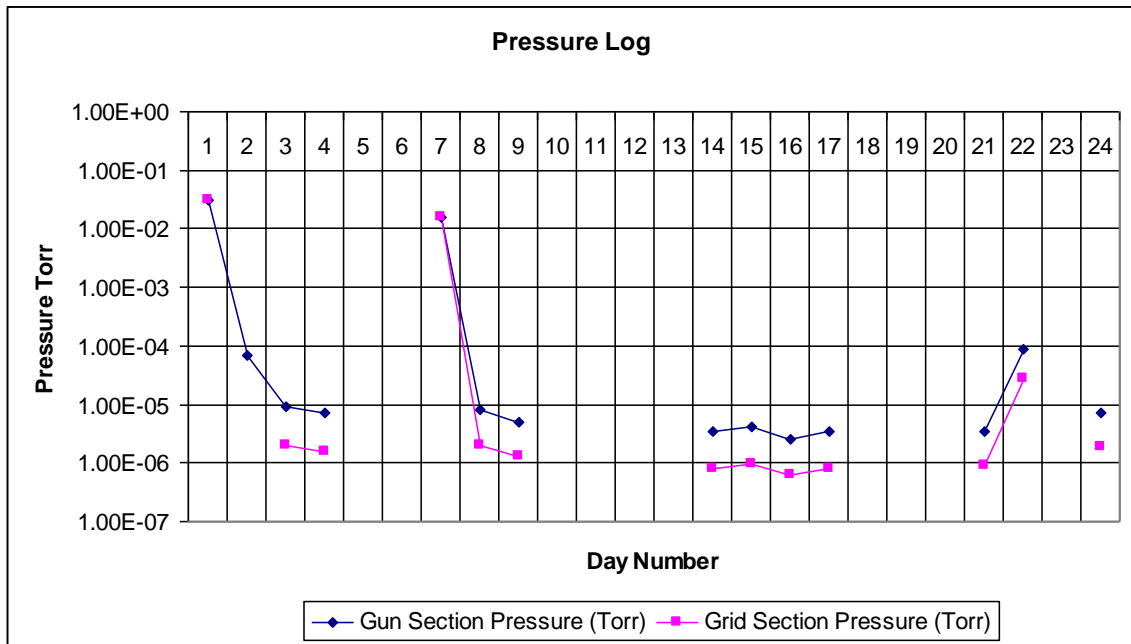
Figure 2.2 Beam Line Pressure Log

Pumping down the system an average base pressure on the order of 10^{-6} Torr can be realized after approximately two days. For the initial pump down of the system in Madison, as depicted in above figure 2.2, more time was required as the system had been disassembled and transported. This meant that the system had been up to air for some time and all the dirt and moisture had to outgas before base pressure could be reached. The grid section is consistently at a lower pressure simply due to the presence of a much larger turbo pump on that side of the device. Gaps in the pressure log respond to times that the system was sealed and pumping stopped. The log records the lowest pressure of the day, thus turbo pumping resumed the 14th and pressure was recorded at days end.

Of more concern is the ability to quickly and easily derive information about the quality of the beam focus and placement. Information about these quantities is obtained from two detectors present in the beam line. The first, called aperture plates, are located just after the horizontal sweep plates. These provide information about the beam location and some information about possible focus before the beam passes through much of the drift pipe and well before the target. This information is most useful in determining if the beam is well centered. It consists of four conductive plates on which individual currents can be read if struck by beam.

16

The most important information about beam focus at the target and location in the test stand is supplied via the focus detection grid. It is a wire grid with fourteen individual outputs which can be used to sense currents driven on the detection wires due to beam impact. This allows location of the beam in a Cartesian based coordinate system. Unfortunately the unused wire outputs must be grounded to prevent charge build up which would lead to beam deflection and arcing between grid wires. The wires in use must be run through current to voltage converters before reading for the same reason. Presently it is impossible to read more than three outputs reliably as only three current to voltage converters proved reliable. This requires the system operator to follow a detailed procedure for focusing the beam and rely on intuition developed from experience. This is not ideal for ease of use by new operators and can lead to faulty conclusions. Ideally all outputs from both detectors could be fed through a set consistent current to voltage converters and read into a DAC enabling graphical computer display of beam condition.

2.2.1   Operation of Beam Line Test Stand

Proper operation of the HIBP calls for a well focused beam at the entering edge of the target plasma. Work with the beam line test stand concluded that a beam of 1cm in diameter is achievable; however, it may be possible to improve this figure through following proper beam focus technique and detailed observation.

Estimation of the size of the beam on target is accomplished via information obtained from the detection grid. Ideally this grid is very near the target to give accurate data. Operation on the test setup required the use of a TREK power supply biasing the vertical sweep plates and controlled as to sweep the beam across several wires in the detection grid. Wires in the detection grid were connected to current to voltage converters. Thus when an ion from the beam hit a wire it would induce a current which could be read as an output voltage on an oscilloscope. The current to voltage converters were important as not to allow the wires to develop a static charge and thus an electric field which would deflect the ion beam. Observation of currents on various grid wires enables the determination of the size and position of the beam.

The grid, which is depicted below in figure 2.3, is simply a rectangular array of wires. Currents can be read off of individual wires as a beam is swept across. Knowledge of wire spacing and beam transit time as observed by the rise and fall of signal as the ion beam passes over a pair of parallel wires enables determination of beam size and location. Currents should be read through current to voltage converters to reduce error. If simple resistive elements are used to read currents the grid wires will achieve some potential and cause some deflection of beam around individual wires. If any wires are unused they must be grounded to prevent charge build up and potential arcing.
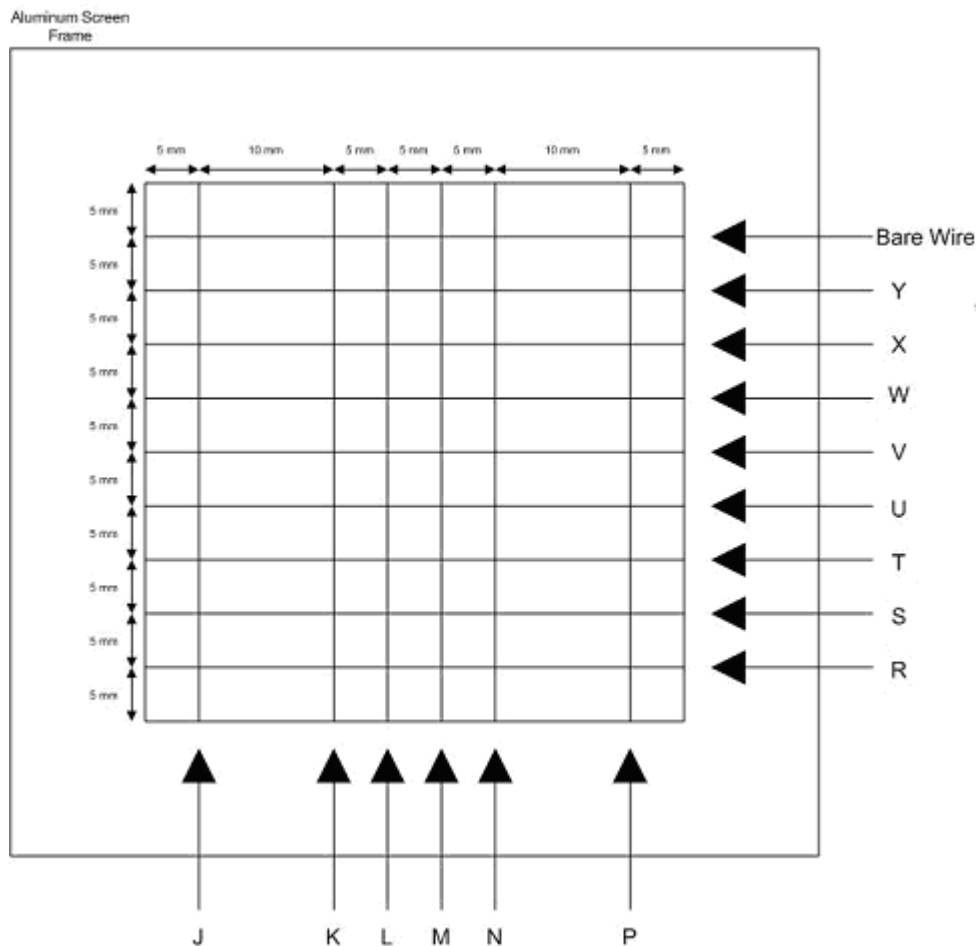

Figure 2.3 Beam Detection Grid
        http://hsxhibp.ece.wisc.edu/wiki/pmwiki.php?n=HIBP.Beamline

2.2.2 Aperture Plates & Gun Box Alignment

If conditions for a beam are set, but none is observed at the detection grid alignment of the gun box may be necessary to ensure the beam is able to reach the target and not slamming into some portion of the vacuum hardware. Located just after and in the same housing as the horizontal sweep plates the aperture plates, see figure 2.4, are four metal plates which form a rectangular aperture at their center. By means of reading voltages on a specific plate it is possible to ascertain the general direction of the beam and to determine if it is extremely diffuse. Reading voltages from resistive elements which indicate ion current striking a plate is not ideal. This is for the same reason that reading voltages on the grid detector wires by resistors is not recommended, the plate will achieve some potential and thus influences the beam direction by electric field action. However, results with resistors were sufficient to steer the beam to the detector grid.

The physical adjustment of the position of the Gun Box is often required upon the installation of a new source, or if the Gun Box has been removed from the beam line and must be reattached. In the case of source replacement, alignment is required as the source axis is unlikely to exactly coincide with the axis of the beam line. Even if a source alignment tool is used.

The following procedure will make it possible for the ion beam to reach the detection grid:

1. Ensure all vacuum and High Voltage connections are secure.
2. Heat the ion source according to the source heating procedure. If this is a new source it is very important that the break in procedure for new sources be followed. If not source life will be very short.
3. Take the leads from the Split Aperture Plate feed through and connect each to a 1MΩ resistor which is grounded at the other end. It is often convenient to attach one end of the resistor to the vessel wall by wrapping it around a bolt and tightening it down with an extra bolt.
4. Set up to measure the voltages across each of the four resistors.
5. When the source is at full current, approximately 6A, and the High Voltage supplies are biased for a relatively well focused beam begin observing the voltages present on the split plates.
6. By using the vertical and horizontal adjusts on the Gun Box, vary the aim as to minimize the voltages present on the split plates. Ideally they will all become zero, but this may not be possible if the focus is poor.

7. It is suggested that a scale be affixed or some other positional reference be employed as to keep track of the Gun Box spatial location.
8. Once the Split Plate voltages are minimized, remove the resistors and directly ground the split plates.
9. Turn attention to the detection grid and attempt to ascertain the position of the beam on the grid.
10. If the beam is well centered alignment is complete. If not, apply DC voltages to the sweep plates to better center the beam. Continue until satisfied.
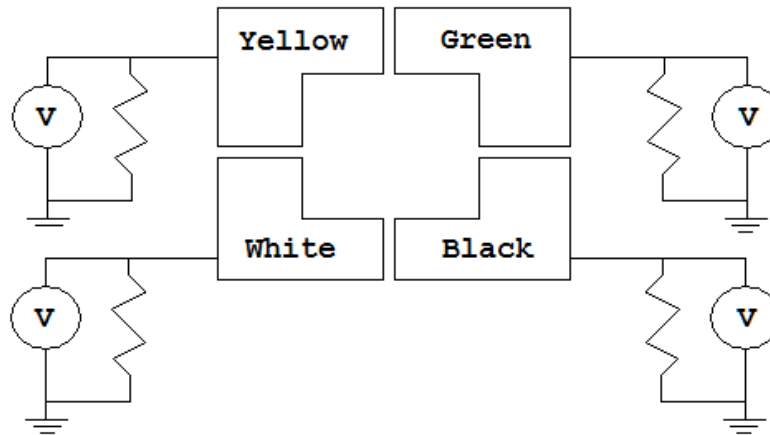
Figure 2.4 – Aperture Plates

2.2.3   Procedure for Running a Beam

Since running a well focused stable ion beam is such an important aspect of beam probing it is appropriate to briefly review the procedure for running a good beam on the beam line test stand as this will be basis of the system implemented on HSX.

1. Pump the system down to at least 10^{-5} T
2. Ensure gate valve dividing Gun and Grid Sections is open
3. Ensure grounds on unconnected wires to prevent charge build up
4. High voltage supplies are set to lowest output before turning on
5. Turn on all power supplies and function generator
6. Function generator set to sine wave with $5V \leq V_{pp} \leq 7V$ & $500kHz \leq f \leq 800kHz$
7. Turn on power amplifier from zero position
8. Raise the source bias from 3kV to 5kV
9. Raise the power amplifier until the ammeter reads 0.25A
10. Raise power at about an amp per quarter hour until nearly 6A is read
11. Raise the extractor and lens bias supplies to 5kV simultaneously
12. Raise source bias supply to desired Pierce voltage
13. Raise other supplies not exceeding a 10kV difference between supplies
14. Adjust extractor and lens bias while watching for detector signal
15. If no focus pattern appears check gun box alignment

Figure 2.5 – Electrical Diagram of Gun
        http://hsxhibp.ece.wisc.edu/wiki/uploads/HIBP/SourceElectricalDiagram

2.2.4   Turning off the Beam

The beam is very simply turned off by first decreasing the voltages on all of the supplies in steps. This way a voltage difference between any two supplies will not exceed 10kV and the risk of arcing is removed. Observe in figure 2.5 that the Pierce plate and extractor are situated very close to one another. If a large enough potential is allowed to exist between them arcing is likely. Placing a limit on this potential difference as part of procedure essentially removes this risk. Decrease the current through the source at a similar rate to which it was raised. This will prevent thermal shock and damage to the source. Finally turn off all supplies and function generators.

2.3   Action Items

Having successfully achieved the objectives laid out at the start some issues remain to be addressed before the beam line is integrated into HSX. Many of these concern accurate measurements and indicators of beam condition. The gauge readings of much of the high voltage control equipment are unreliable and either replacement of existing supplies or careful calibration will be necessary. Replacement of old ionization gauges is also practical. Most importantly, the creation of a computer graphics based read out of beam information at the focus grid will allow a far better understanding of beam behavior and ease of operation.

3. COMPUTER SIMULATION

3.1 Simulation Application

The conditions present in HSX allow for the reconstruction of $\vec{E}$ within a plasma based upon HIBP measurements. Deflections in ion trajectories can be observed and compared. Trajectories can first be established for the magnetic field $\vec{B}$ of the stellarator only, without plasma. Then trajectories can be established for a specific plasma and thus a specific electric field. The trajectories observed in the absence of an electric field can be compared to those predicted for the same condition, as the magnetic field is well known and can be simulated accurately. Then deflections in trajectories produced by a modeled electric field can be compared to the deflections produced by the actual electric field of a plasma in HSX. If a modeled electric field accurately describes deflections over a range of sweep angles for given plasma and beam parameters it is a good description of what is actually going on.

There is, as yet, no actual data for the deflections induced in ion trajectories by electric fields present in plasmas run in HSX. However, knowledge of magnetic conditions within HSX allow for predictions of likely electric field shape. This is because the magnetic flux within HSX is well known and where the gradients in magnetic flux are the largest the greatest electric field influence is expected. This enables a likely guess which can be called the base state electric field. This base state field can be taken as data until such time that real data is available. The deflections in ion trajectories from this base state electric field produced by guessed electric fields can be used to investigate simulated plasma. If a guessed electric field can be modified to reproduce the impact locations on a detector line of base state ion trajectories then a reasonable reconstruction of the electric field will have been achieved. Thus when actual trajectory data becomes available reconstruction will enable a very accurate representation of $\vec{E}$.

3.2 Early Work

Early investigations into expected trajectory deflections due to electric fields present in plasmas were undertaken at UW, Madison by C. H. Stallings [9]. Experiments were conducted on cylindrical inertially confined plasma columns with parameters which only depended on radius. The method passed an electron beam, originating from and detected far outside the field region, through the plasma and observed deflection by internal $\vec{E}$ fields. The use of an electron beam is not appropriate to use in probing HSX primarily due to the infinitesimal mass of the electron and the strong confining magnetic field present, which was not a factor for Stallings. These factors would combine to produce a gyromagnetic radius several orders of magnitude smaller than for a heavy ion and consequently no region of interest could be sampled.

The work developed an analytic model for an electric field composed of thin shells such that $\vec{E} = 0$ outside of the range $r + \Delta r$. Essentially an electron with known energy is deflected through an angle as it passes through a shell upon entering the plasma then by symmetry that angle is doubled as the electron leaves the plasma passing through the shell once more. The method composed a predicted angle of deflection by integrating over all the thin shell electric fields which composed the plasma region. Thus $\vec{E}$ was taken as a function of r alone and was present inside the integral. Via an inversion similar to that of the Abel inversion it was shown possible to obtain information on the potential function which had given rise to the electric field.

Further expanding upon the notion of a layered $\vec{E}$ the most recent models for such trajectory deflections with relevant application to HSX were conducted by Xi Chen [10] of RPDL. The method employed by Chen differed in that $\vec{E}$ was assumed a constant within any given layer and the thickness of these cylindrical layers were predefined by the penetration of an ion trajectory into the plasma column.

3.3 Simulation Methodology

3.3.1 Simulation Simplifications

Some important simplifications to real geometries have been made, though the design of this work has been to enable ease of application of models and simulation techniques to the real HSX system. First the simulated system has been reduced to that of a cylindrically symmetric geometry. This can easily be readapted for use in the non cylindrical conditions of HSX via modification of the modular field functions present in the trajectory codes. Where the main trajectory function calls sub functions to determine values of electric and magnetic fields at any location. Substitution of these functions would allow the trajectory function to return outputs using actual HSX fields. Second the electric field has been divided into five annular regions which are linearly dependent upon radius. Further, the electric field is continuous over this domain, which is defined for the known average plasma extent in HSX. Chen worked with regions of constant electric field which had discontinuities at the layer boundaries.

The magnetic fields used in simulation are based upon data from HSX and fit to a polynomial function, where this again is a function that could easily be changed in the future. The magnetic field used is fit to the field data obtained from HSX code for the box-port plane where the HIBP system will eventually be implemented. The HSX field data for this location is displayed below, in figure 3.1, where zero meters lies on the central axis of the machine and B_z is the field component normal to the plane of the box port where the HIBP system will be installed. See figure 3.11 which shows a cross section of the HSX box port. The distorted rings depict flux surfaces in HSX with the coordinate origin at the center. It is in this plane, in this region, where all trajectory simulations take place [10].

Primary attention is paid to the B_z field component, just as in a tokamak, where beam trajectories lie essentially in or near a plane. In tokamak geometry the z-direction aligns with the toroidal direction and the beam trajectories lie close to a plane of constant toroidal angle. In this case, the perpendicular to the box port aligns with the helical axis of HSX making the direction of B_z appear to be somewhat arbitrary, but the ion trajectories effectively lie in the plane perpendicular to B_z, just as in a tokamak. For

24

regions outside of this range the magnetic field falls off very rapidly and can be considered zero [10].
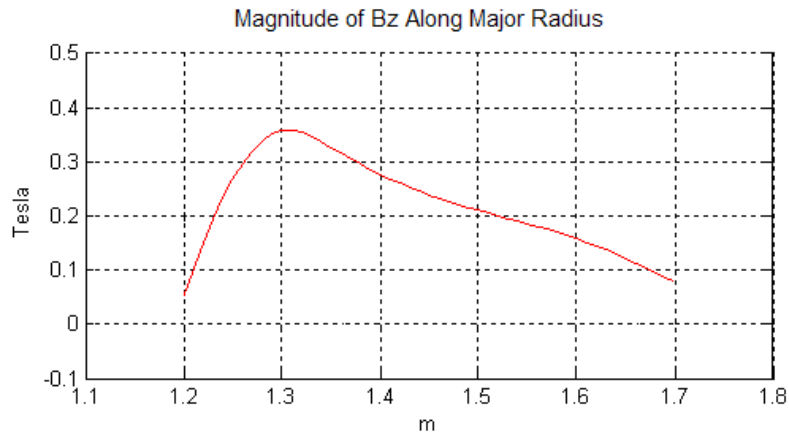

Figure 3.1 Real Magnitude of B$_z$ Along Major Radius in Box-port Plane [10]

The range of injection angles studied was limited. For $\theta_I < -13^o$ the beam looped around outside of the plasma region where $\vec{E}$ was defined as zero and exited rather near the ion gun. For angles $\theta_I > -3^o$ the ion trajectories did not reach the region of interest either, having been curved away by the magnetic field. That is for angles outside this region, trajectory simulations experienced purely magnetic influences and the ion path did not cross into the electric field region as depicted in figure 3.3 by the five central annular regions. The Cs - 133 ion beam with an initial energy of 10kV was settled upon to coincide with elements of the work undertaken by Chen [10]. This beam provided the best penetration in the layered model employed for the low beam energies desired. Through exploration of the same beam parameters it is hoped that the influences of electric field models can be better understood.

3.3.2 Simulation Procedure

3.3.2.1 Establish a Base State Electric Field

Objective: Relate the injection angle θ_I to a hit location as in table 3-1
Input: $\vec{E}(x, y)$ Base State
                  θ_I the Injection Angle

Outputs: Detector Hit Location (x, y)

Table 3-1: Relate Injection Angle to Hit Location

θ Injection Angle in Degrees	Hit Location
θ_1	x_1 y_1
θ_2	x_2 y_2
θ_3	x_3 y_3

3.3.2.2 Trajectory Function

Objective: Return the trajectory of an ion
Inputs: θ_1 & Starting Point

$\vec{E}(x, y)$ Guess

$\vec{B} = \langle B_x = 0, B_y = 0, B_z \rangle$

Beam Energy

Outputs: Ion Detector Hit Position
                Ion Energy

1. Choose Starting Point (x, y) at outer edge of the field region where is $\vec{B}$ small or close to zero.
2. Determine initial ion velocity from beam energy where the direction of $\vec{v}_1$ is known from injection angle.

$$ KE = \frac{1}{2}mv^2 \rightarrow v_1 = \sqrt{\frac{2KE}{m}} $$

3. Step to the next point (x_2, y_2)

First step only
$$ \vec{\ell} = \vec{v}_1 dt = \langle v_1\hat{x}, v_1\hat{y}, 0 \rangle dt $$
$$ \vec{\ell} = \langle v_1 dt\hat{x}, v_1 dt\hat{y}, 0 \rangle $$

Step Out Far
$$ x_2 = x_1 + v_1\hat{x}dt $$
$$ y_2 = y_2 + v_1\hat{y}dt $$

4. Return to midpoint $$ \left(x_{Mid}, y_{Mid}\right) = \left(\frac{x_1 + x_2}{2}, \frac{y_1 + y_2}{2} \right) $$

5. Lookup $\vec{E}(x, y)$
6. Obtain Unit Normal at $\left(x_{Mid}, y_{Mid}\right)$

Define the Unit Vector in the Direction of the Gradient
This is the direction we will step into

26

7. Obtain $\vec{E}(x_{Mid}, y_{Mid})$
8. Obtain $\vec{B}(x_{Mid}, y_{Mid})$
9. Obtain the new velocity vector $\vec{v}_2$

$$\vec{F} = m\vec{a}$$

$$\vec{F} = q\vec{E} + q(\vec{v} \times \vec{B})$$

$$\vec{a} = \frac{1}{m}\left[q\vec{E} + q(\vec{v} \times \vec{B})\right]$$

$$\vec{v}_2 = \vec{v}_1 + \vec{a}dt$$

$$\vec{v}_2 = \vec{v}_1 + \frac{q}{m}\left[\vec{E} + \vec{v}_1 \times \vec{B}\right]dt$$

$$\vec{v}_2\hat{x} = \vec{v}_1\hat{x} + \frac{q}{m}\left[E\hat{x} + (v_1\hat{y})(B\hat{z})\right]dt$$

$$\vec{v}_2\hat{y} = \vec{v}_1\hat{y} + \frac{q}{m}\left[E\hat{y} + (v_1\hat{x})(B\hat{z})\right]dt$$

10. Determine Where the next point will be
11. Move back to midpoint and resolve $\vec{E}(x_{Mid+n}, y_{Mid+n})$ and the new $\vec{a}$ to get the new velocity of the ion. Repeat till intersect with detector line

3.3.3 Base State Construction and Predicted Deflection

The base state is the assumed $\vec{E}$ model for which trajectory calculations are run to determine the precise detector locations. The objective is to relate the injection angle θ_I at a given beam energy to the location hit by the ion trajectory on a given detector line. Thus a table can be generated and used as data to compare the later trajectories produced by guessing possible electric fields. The key concept of base state $\vec{E}$ is that if it is what is really present in the plasma then we will have the ability to reconstruct the actual potential profile.

Defining a reasonable base state for the system requires knowledge of the conditions present in HSX. It is expected that the strongest $\vec{E}$ will be present where temperature gradients are steepest. Previous simulation work by Chen suggests a potential profile which is parabolic and the known magnetic flux profile appears parabolic as well. Using the notion employed by Chen that $\vec{E} = -k\nabla\psi$, where ψ is plotted in figure 3.2, it is reasonable to define a piecewise linear model for $\vec{E}$ which is greatest in magnitude

27

where ψ is changing most rapidly. Though, in the absence of real data determination of base state $\vec{E}$ is substantially open.
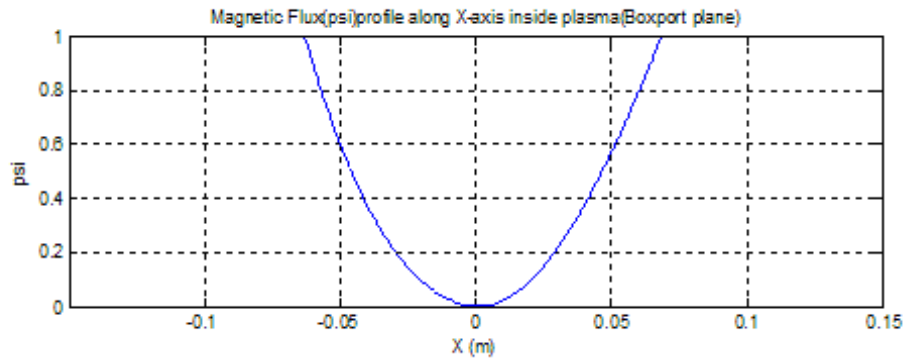

Figure 3.2 ψ Profiles Along x-Axis Inside Plasma in Flange Coordinates [10]

To determine the likely location of a beam detection grid which will be used to measure deflection in trajectories it is first helpful to simulate with only the magnetic field as it is this field which will dominate the likely trajectories. Errors in energy conservation were used to gauge the error in the code. Generally for a reduction in time step of one order of magnitude it was possible to reduce the error in the code by the same. However, for very small time steps error reduction slowed appreciably and computation time increased dramatically. Thus a compromise between reasonable accuracy and practical computation times which were required for study of several injection angle sweeps forced compromise. The error in simulation while in magnetic geometry only was generally quite small, as can be seen in Table 3-2. This table gives the ion hit location and percent energy error using a 10ns time step when only magnetic field is present.
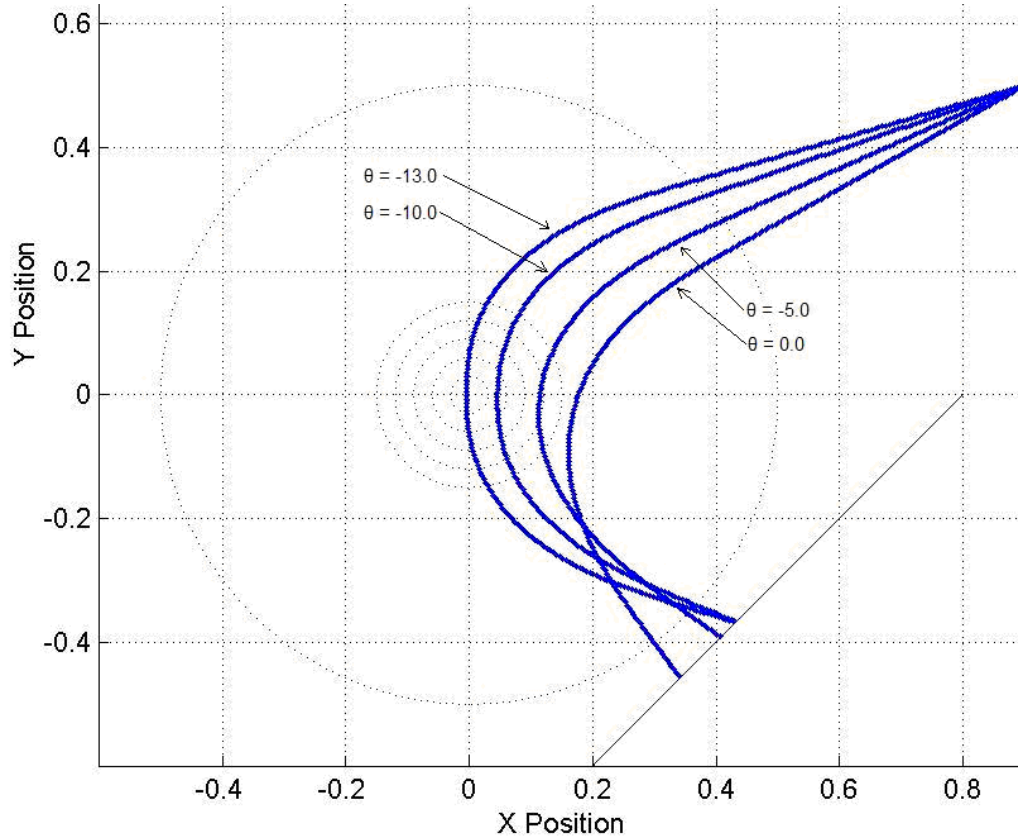
Figure 3.3 Cs - 133 Ion Trajectories for $\vec{E} = 0$ the Magnetic Field Only Condition with Beam Energy 10kV and Injection Angles θ = -13°, -10°, -5°, 0°

Table 3-2: Initial Data for $\vec{E} = 0$ Used to Estimate Detector Locations

θ_L	x_{Hit}	y_{Hit}	Percent Error	$dt = 10^{-t}$
-13.0	4.4100e-01	-3.5932e-01	2.4262e-01	8
-12.0	4.3557e-01	-3.6445e-01	2.3185e-01	8
-11.0	4.3927e-01	-3.6125e-01	2.3061e-01	8
-10.0	4.4052e-01	-3.5950e-01	2.9427e-01	8
-09.0	4.4103e-01	-3.5912e-01	2.2830e-01	8
-08.0	4.3894e-01	-3.6118e-01	2.2591e-01	8
-07.0	4.3353e-01	-3.6689e-01	2.2131e-01	8
-06.0	4.2448e-01	-3.7601e-01	2.1400e-01	8
-05.0	4.1281e-01	-3.8790e-01	2.1026e-01	8
-04.0	3.9893e-01	-4.0115e-01	1.9238e-01	8
-03.0	3.8485e-01	-4.1563e-01	1.7952e-01	8

The next step is to define a likely electric field which will induce measurable deflections. The order of magnitude was set at a maximum of 10^5 $^V/_m$ to coincide with fields producing noticeable trajectory deflections [10]. The electric field is taken as

29

static because the time scale for an ion to traverse the plasma is much smaller than that associated with expected field variation. The radius of electric field extent was estimated to be the plasma minor radius. This region is divided into five annular domains; see the central region of figure 3.3. The electric field is pegged to preset values on these rings. These points determine the magnitude of the electric field at 6, 9, and 12cm with the ends pegged to zero at 3 and 15cm; see figure 3.4. The electric field is allowed to vary linearly with radius in each annular domain and to be continuous across domains. This differs from Chen's constant values for electric field in a layer and avoids the discontinuities such an approach creates.

It was hoped that limiting such discontinuities would reduce energy error. Comparison of this method, employing a time step of 10^{-9}s, with energy conservation results presented by Chen, using a time step of 10^{-11}s, resulted in energy errors on the same order of magnitude [10]. Detailed data on code energy error for the base state electric field is presented below in table 3-3 and plotted as a function of injection angle in figure 3.6. Note for time steps of 100ns and smaller the shape of the energy error as a function of injection angle does not change and shifts downward.

There are important considerations to take into account when choosing a detector location for further analysis. First is the amount of deflection from the $\vec{E} = 0$ condition to the measurable base state electric field condition. Second is how much error is present in the code at a given injection angle. Last is to determine if the trajectories are simple. That is to say trajectories from different injection angles cross at some point in the field region which leads to more complex trajectories. Generally it is best to rely on the simplest trajectories for building a field model. This means that the detector line present in figure 3.3 should be moved in very close to the electric field region and should lie about 20cm from the origin. Greater than this distance trajectories begin to cross and the sweep patterns become more complicated.

Running a sweep of trajectories with injection angles varying by one degree from -13° to -3° for the magnetic field only condition and for the base electric field state condition allows for comparison of hit points as a function of injection angle. Figure 3.5 plots the distance between the hit points along the detector line, as depicted in figure 3.3

and 3.7, for the two cases, respectively. Figure 3.5 clearly shows that the distance between hit points for these two conditions is a strong function of injection angle.
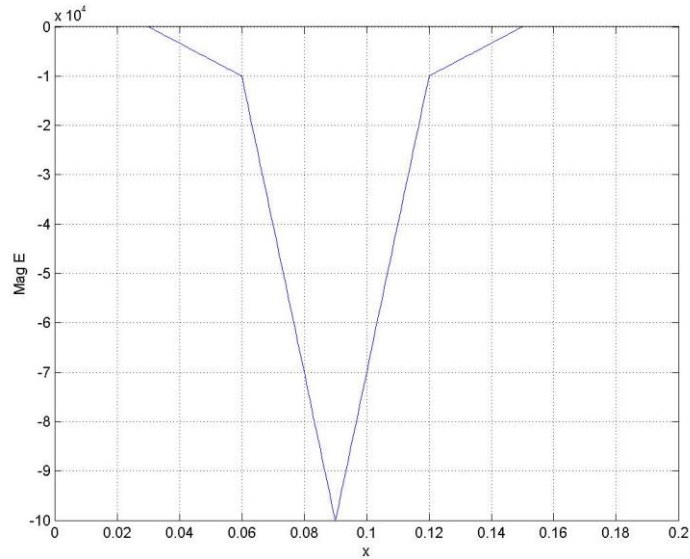

Figure 3.4 Base State Electric Field with Set Values at Radial Distances 6, 9, and 12cm and the ends pegged to zero at 3 and 15cm
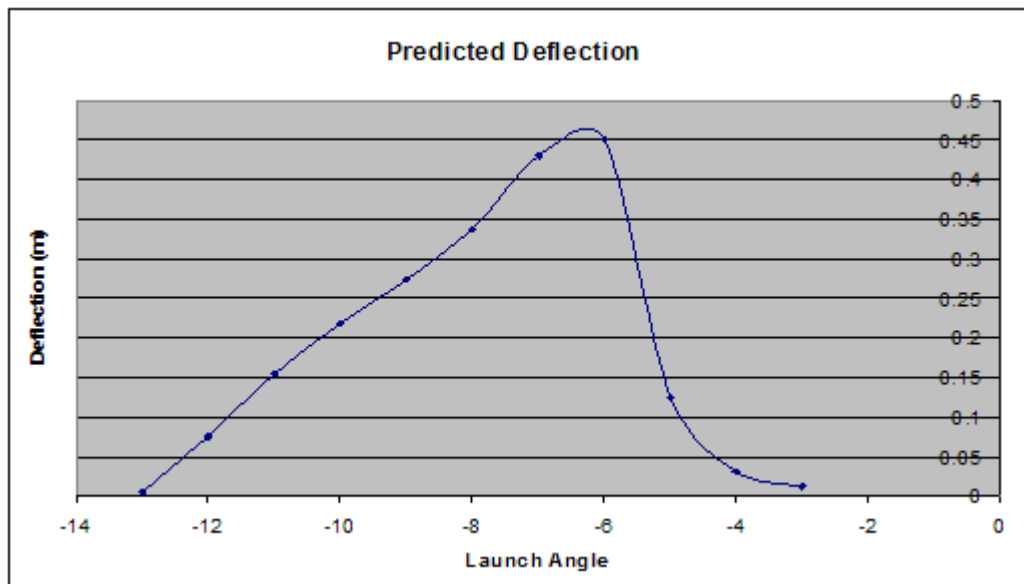

Figure 3.5 Predicted Distances Between Hit Points Along Detector Line from the Base State Electric Field Condition to a Test Electric Field of Zero
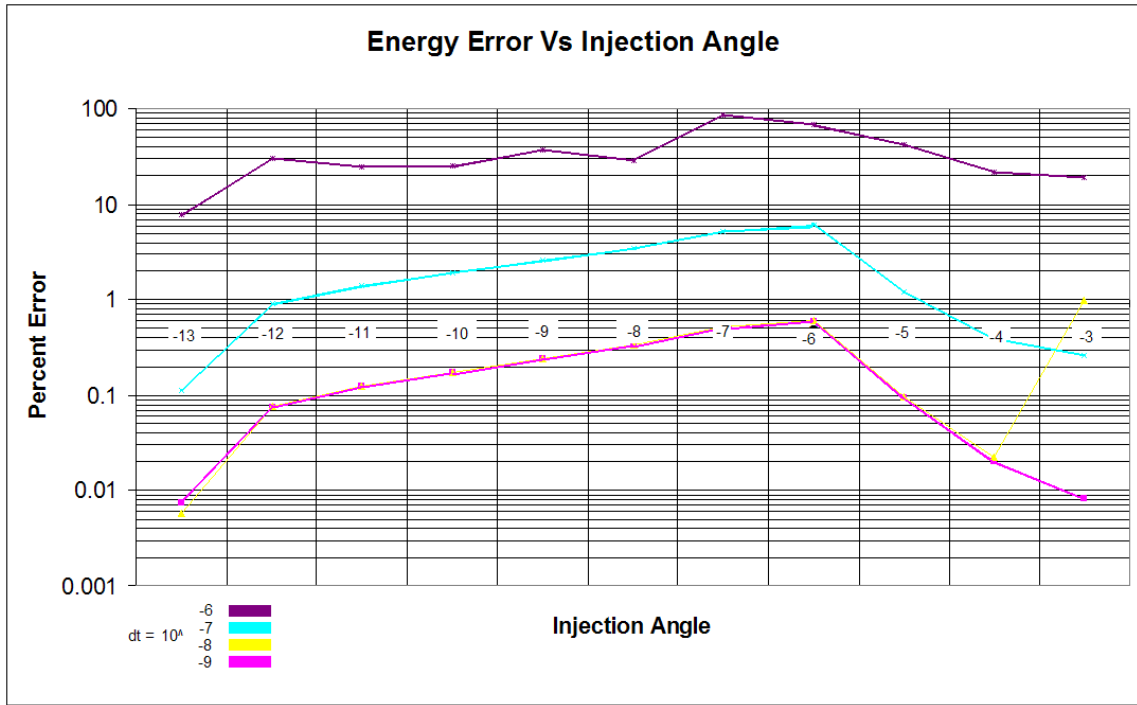
Figure 3.6 Percent Energy Error as a Function of Injection Angle for Base State Electric Field Plotted for Four Decreasing Time Steps

Table 3-3: Percent Energy Error for Base State Electric Field Decreases with Shrinking Time Step

| θ_I (Degrees)	Percent Error dt = 10^-9s	Percent Error dt = 10^-8s	Percent Error dt = 10^-7s	Percent Error dt = 10^-6s
-13	7.52E-03	5.78E-03	1.13E-01	7.91E+00
-12	7.55E-02	7.70E-02	9.20E-01	3.04E+01
-11	1.24E-01	1.25E-01	1.40E+00	2.47E+01
-10	1.74E-01	1.76E-01	1.90E+00	2.53E+01
-9	2.40E-01	2.42E-01	2.56E+00	3.75E+01
-8	3.35E-01	3.36E-01	3.49E+00	2.88E+01
-7	5.14E-01	5.15E-01	5.26E+00	8.55E+01
-6	5.95E-01	5.97E-01	6.17E+00	6.88E+01
-5	9.57E-02	9.78E-02	1.19E+00	4.21E+01
-4	2.02E-02	2.19E-02	3.93E-01	2.19E+01
-3	8.29E-03	9.92E-01	2.62E-01	1.93E+01
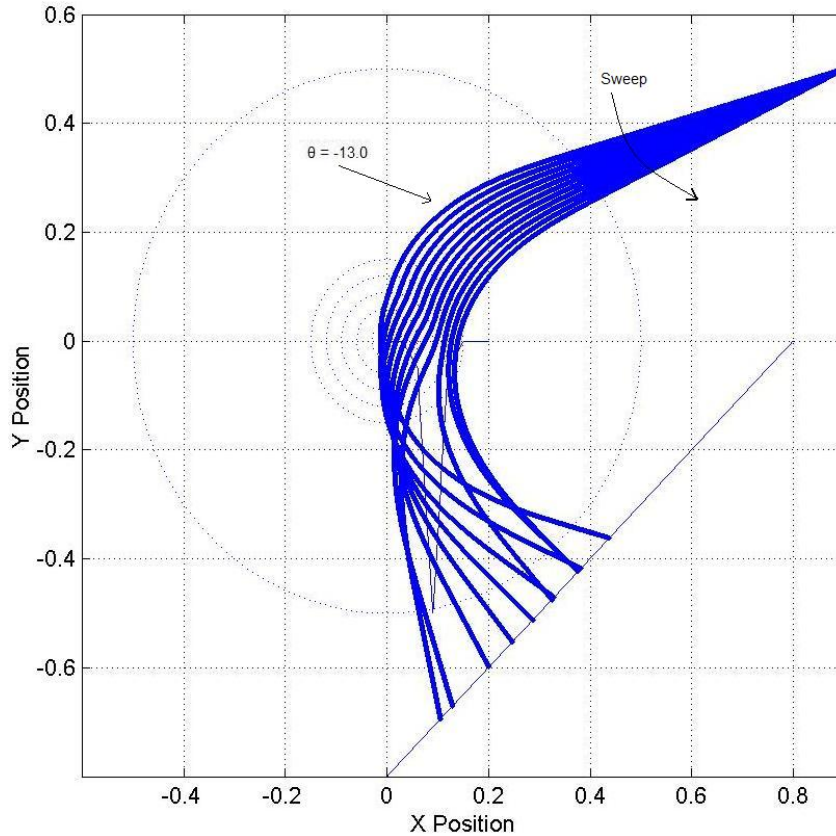
Figure 3.7 Sweep of Base State Electric Field Trajectories Sampling the $\vec{E}$ Region Injection Angles Incremented by One Degree from θ = -13° to -3°

Note in the above figure 3.6 that the error converges at time steps of 10ns and 1ns so adding a variable time step would result in a large reduction in computing time without hurting the reliability of trajectory calculation. Another clear pattern is visible, that is error rises substantially the more the electric field region is sampled. This is expected as the longer an ion is in the electric field region the more acceleration it can experience. For the injection angles $-8 \leq \theta_I \leq -4$ the errors rise sharply and substantially; however, it now must be determined if this is the most interesting area. Through running several sweeps of injection angles it is possible to determine which trajectories would be the most promising to use to in determination of detector locations. Looking at a detailed section of the previous sweep shows which trajectories are bent the most.
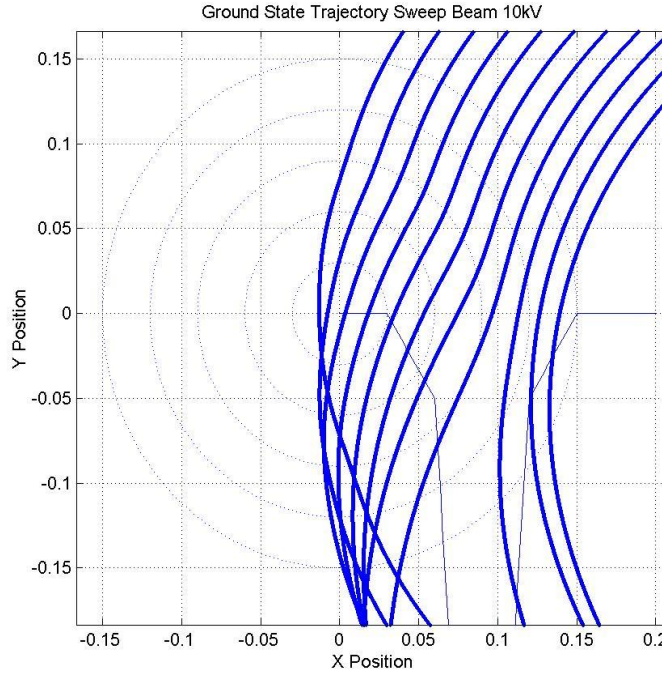
Figure 3.8 Center Detail Sweep of Trajectories Sampling the $\vec{E}$ Region $\theta = -13^o$ to -3°

Taking figures 3.7 and 3.8 together we have a good view of the trajectories which sample the electric field region. A strong lens is observed at about (0, -0.2) in the figures for injection angles smaller then -6 degrees. Figure 3.8 displays how the trajectories are bending just prior to this point. Once an ion is launched at -6 degrees, the fourth trajectory from the right, it samples the high magnitude electric field region enough to experience significant deflection from the purely magnetic trajectory. If you carefully observe each trajectory as it enters the high field region it experiences a marked bend. This region exerts the most influence due to its large magnitude. Further understanding of the influences of electric field magnitude on deflection can be explored by retaining the same shape but altering the magnitudes of the electric field regions; figure 3.9 plots this.

Table 3-4: Base State Field with 10kV Beam

θ_L	x_{Hit}	y_{Hit}	Percent Error	$dt = 10^{-t}$
-13.0	4.3811598e-01	-3.6191770e-01	7.52E-03	9
-12.0	3.8235195e-01	-4.1771299e-01	7.55E-02	9
-11.0	3.2939899e-01	-4.7061994e-01	1.24E-01	9
-10.0	2.8775440e-01	-5.1232609e-01	1.74E-01	9
-09.0	2.4694668e-01	-5.5313588e-01	2.40E-01	9
-08.0	2.0068957e-01	-5.9942493e-01	3.35E-01	9
-07.0	1.2901687e-01	-6.7099556e-01	5.14E-01	9
-06.0	1.0527749e-01	-6.9476141e-01	5.95E-01	9
-05.0	3.2460373e-01	-4.7547260e-01	9.57E-02	9
-04.0	3.7662844e-01	-4.2346234e-01	2.02E-02	9
-03.0	3.7646065e-01	-4.2356240e-01	8.29E-03	9

3.4   Trajectory Study

The best way to determine the electric field effects on trajectory deflection is to run several sweeps of ion trajectories for different field configurations. Several sweeps over the same angles as before were preformed and then plotted with each series for a different field configuration. The two figures describing this are 3.9 and 3.5 which plot deflection from base state electric field hit points and deflection from no electric field hit points, respectively. The hit points for no electric field are detailed in above table 3-4. The field was varied by one order of magnitude from one series to another. The results are clear, the more a field region is sampled the greater its influence.

The deflections from the base state demonstrated a strong dependence on injection angle and only a much smaller influence due to electric field, even though the field is greatly altered in each series. This suggests that it may be difficult to separate deflections amongst electric field functions with similar shapes because the magnetic field influences are so strong. This concept is further investigated in figure 3.10 where the distance between hit points found under the condition where there is only magnetic field and hit points found for the same series of electric field profiles studied in figure

3.9 are plotted. All profiles plotted in figure 3.10 demonstrate the same shape with deflections spanning a very wide range. It appears that the magnetic field function dominates the path of ion trajectories.
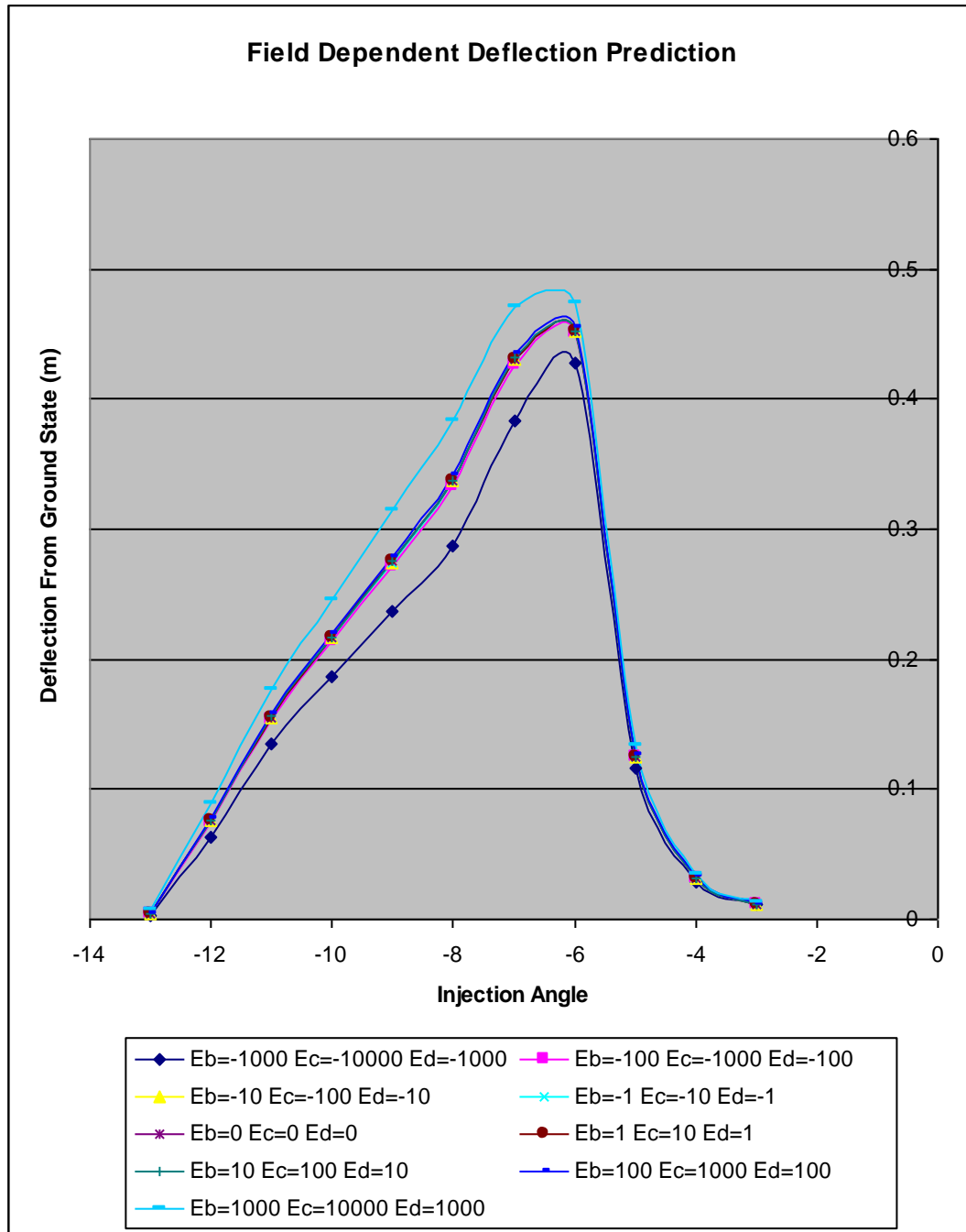

Field Dependent Deflection Prediction

Legend:
- Eb=-1000 Ec=-10000 Ed=-1000
- Eb=-100 Ec=-1000 Ed=-100
- Eb=-10 Ec=-100 Ed=-10
- Eb=-1 Ec=-10 Ed=-1
- Eb=0 Ec=0 Ed=0
- Eb=1 Ec=10 Ed=1
- Eb=10 Ec=100 Ed=10
- Eb=100 Ec=1000 Ed=100
- Eb=1000 Ec=10000 Ed=1000

Axis labels: Deflection From Ground State (m), Injection Angle

Figure 3.9 Deflections from Base State Electric Field Hit Points to Tested Electric Field Hit Points
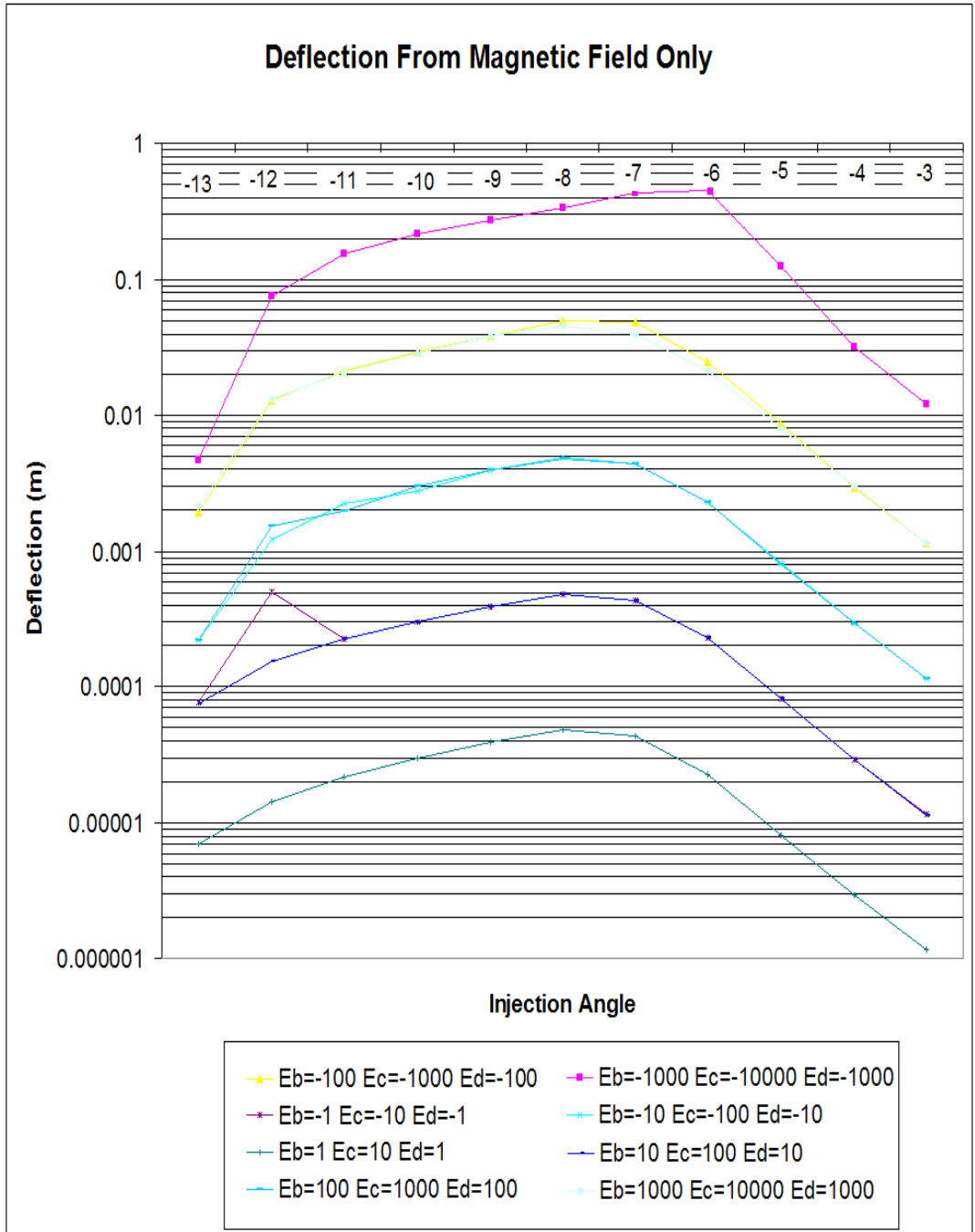
Figure 3.10 Deflections from Zero Electric Field Hit Points to Tested Electric Field Hit Points

3.5   Method for Reconstruction of Electric Field

The trajectory function is capable of determining the location of ion impact given a varied electric field function.   Thus the basic premise for reconstruction requires starting from a reasonable electric field profile.   Then the location of the base state ion impact can be compared to the location of the ion impact due to the guessed electric field.   Through minimization of this distance it is possible to bring a guessed electric field into alignment with the base state electric field.

A code has been created to vary one of the three free parameters in the base state model at a time.   This code requires the recalculation of hit points via the recalculation of the entire trajectory using the variation on the guessed electric field parameter.   This code has proven very inefficient and difficult, yielding only minute changes in distance for large changes in each of the three free parameters in the field model.   These parameters define the magnitude and slopes of the linear regions.   The extremely limited variation makes reconstruction highly unreliable and subject to initial guess.   It is likely that this is due to the small size of deflections from base state trajectories, as seen in figure 3.9 the deflections appear very small for all but the largest electric field functions.
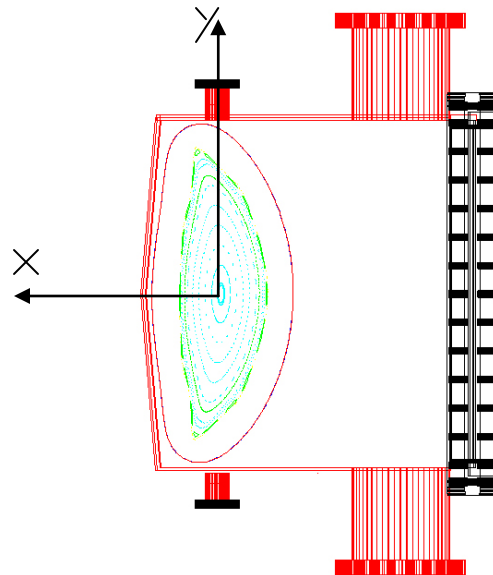

Figure 3.11 Diagram of Box Port Plane Showing Flux Surfaces with Box Port Coordinate Origin at the Center of the Flux Surfaces [10]

4. DISCUSSION AND CONCLUSIONS

4.1 Discussion and Conclusion

The fundamentals for a simple HIBP electric field diagnostic have been brought together for HSX. A body of Matlab codes and simulations have provided the theoretical background and projected behaviors to lay down the required design parameters. Major efforts have been made to relocate and prepare a HIBP system for implementation on HSX as well as to develop procedures and further educate key personal as to the special skills required to achieve good system performance.

The body of code allows changes in several parameters such as: injection angle, initial beam energy, ion species, and detector position. These can be changed and trajectories run allowing sampling of different regions of plasma. This work has served to produce a code which allows for simple substitution of functions which define the fields present and will aid in the future accurate simulations of electric field deflection effects on HSX. Improved models for the base state field as well as more efficient optimization techniques will be required to fully exploit the trajectory calculation functions for HSX.

4.2 Future Work

4.2.1 Adapted Trajectory Function

Objective:	Return the trajectory of an ion
Inputs:	θ_I & Starting Point
	$\vec{E}(x, y)$
	$\vec{B}$ Defined by HSX Code
	Beam Energy
Outputs:	Ion Detector Hit Position
	Ion Energy

Again choose Starting Point (x, y) at outer edge of the plasma where is $\vec{B}$ defined by HSX Code. Just as before determine initial ion velocity from beam energy and the direction of $\vec{v}_1$ from the injection angle. Then just as the former trajectory function calculated step out far using this velocity then return to the midpoint. Then here at the midpoint where field calculations are made it is possible to do something interesting.

When constructing a base state create a scalar potential function instead of an electric field function. It is peculiar that in HSX the magnetic flux as a function of space is well known and thus the surfaces of constant flux are well defined. Then instead of using the negative of gradient of the potential function it is possible to correlate the potential at a position with the flux. Then when calculating a new acceleration look up $\psi(x_{Mid}, y_{Mid})$ at the point and interpolate $\phi(x_{Mid}, y_{Mid})$. The direction can be defined by the gradient of the flux as found by:

$$\vec{n} = \frac{\frac{\partial \psi}{\partial x} \hat{a}_x + \frac{\partial \psi}{\partial y} \hat{a}_y}{\sqrt{\left(\frac{\partial \psi}{\partial x}\right)^2 + \left(\frac{\partial \psi}{\partial y}\right)^2}}$$

This is the direction which the ion is accelerated and thus the direction that the trajectory will step into. Then calculate $\vec{E}(x_{Mid}, y_{Mid})$ by:

$$E_x = \frac{\phi_2 - \phi_1}{\ell} \frac{\frac{\partial \psi}{\partial x}}{\sqrt{\left(\frac{\partial \psi}{\partial x}\right)^2 + \left(\frac{\partial \psi}{\partial y}\right)^2}} \qquad E_x = \frac{\phi_2 - \phi_1}{\ell} \frac{\frac{\partial \psi}{\partial y}}{\sqrt{\left(\frac{\partial \psi}{\partial x}\right)^2 + \left(\frac{\partial \psi}{\partial y}\right)^2}}$$

Calculation of the new acceleration can then be completed by obtaining $\vec{B}(x_{Mid}, y_{Mid})$ from codes written for HSX. Then the calculations are repeated just as in the older trajectory function.

REFERENCE

[1] F.S.B. Anderson, A.F. Almagri, et al., "The Helically symmetric experiment, (HSX) goals, design and status", *Fusion Technology* 27, 273 (1995)

[2] T.P. Crowley, "Rensselaer Heavy Ion Beam Probe Diagnostic Methods and Techniques", *IEEE Transactions on Plasma Science.* Vol. 22, No. 4, August 1994

[3] http://www.hsx.wisc.edu/construction.shtml

[4] http://www.hsx.wisc.edu/

[5] Shah, "Measurement of Potential Profiles in the MST RFP Using a HIBP," RPI. Troy, NY PhD Thesis 2002

[6] Prof. D. Steiner, "Course Notes: Introduction to Fusion Devices and Systems" RPI. Troy, NY

[7] Lei, "Measurement of Core Potential & Density Fluctuations on the MST RFP Using a HIBP," RPI. Troy, NY PhD Thesis 2002

[8] I.H. Hutchinson, "Principles of Plasma Diagnostics", 2nd Edition, Cambridge University Press, 2002

[9] Stallings, C., "Electron Beam as a Method of Finding Potential Distribution in a Cylindrically Symmetric Plasma", Journal of Applied Physics, Vol. 42, No. 7, June 1971

[10] X. Chen, "Determining the Electric Field in a Plasma by Measuring the Deflection of an Ion Beam," RPI. Troy, NY Masters Thesis December 2007